Periods of High Intensity Solar Proton Flux

Michael A. Xapsos, *Senior Member, IEEE*, Craig A. Stauffer, Thomas M. Jordan, *Member, IEEE,*
James H. Adams, Jr. and William F. Dietrich

***Abstract*—Analysis is presented for times during a space mission that specified solar proton flux levels are exceeded. This includes both total time and continuous time periods during missions. Results for the solar maximum and solar minimum phases of the solar cycle are presented and compared for a broad range of proton energies and shielding levels. This type of approach is more amenable to reliability analysis for spacecraft systems and instrumentation than standard statistical models.**

***Index Terms*—solar particle event, worst case flux**

I. Introduction

Developing and implementing strategies to deal with the space radiation environment is critical for new robotic and manned exploration initiatives. In order to have reliable and cost-effective spacecraft design and implement new space technologies accurate models that view things from varying perspectives are needed for estimating radiation risks. Underestimating radiation levels leads to excessive risk and can result in degraded system performance and loss of mission lifetime. Overestimating radiation levels can lead to use of excessive shielding, reduced payloads, over-design and increased cost.

Evaluating the risk due to solar particle events is a significant concern for all space missions, especially those away from the protective shielding effects of the Earth's magnetic field. Due to the difficulty in forecasting the occurrence and magnitude of solar particle events [1] probabilistic approaches are widely used to characterize events. In this regard, useful models have been developed to describe cumulative fluences [2-6] and worst case events [7,8] at a given level of confidence over the course of a mission. For the situation of worst case events it is also common to pick a severe event such as the well known one that occurred in October 1989 and assume this is worst case for the mission, as is done in the CREME96 suite of codes [9].

When trying to establish a worst case environment additional information can be required by the space system designer. It is also useful for the designer to know how much total time during the mission that a pre-determined flux level is exceeded. This allows a straight forward assessment of the mission time period during which there should be reliable system or instrument operation. In many instances this is closely related to the design goals of the mission. For example, within the NASA Living With a Star (LWS) program the goal of the Solar Dynamics Observatory (SDO) instrumentation is to capture essentially complete data over 22 72-day periods during its 5 years of operations. This allows for data loss due to planned and unplanned events, the latter of which includes radiation. Another example within LWS is the Space Environment Testbed (SET) payload, which has a full mission success criterion of delivering 95% of the data for 40 weeks out of the 1 year of planned operations. The SET payload will be flown on the US Air Force Research Laboratory's Demonstration and Science Experiment (DSX) spacecraft. Another emerging development is that compact radiation monitors such as QinetiQ's Merlin [10], and ESA's Standard Radiation Environment Monitor (SREM) [11] are being flown with increasing frequency. An application of such monitors is to send out alerts when specified radiation levels are exceeded. Thus, quantitative prediction of the periods of high radiation levels is becoming increasingly important during the mission design phase.

Besides the total time during a mission that a radiation flux level is exceeded, it can also be important to evaluate the longest *continuous* time period that a given level is exceeded. This is significant for evaluating single event effects in microelectronics as well as imagers such as CCDs.

This work develops an approach for analyses of solar proton fluxes that contributes directly to these spacecraft design requirements. It evaluates both the expected total time and longest continuous time during a mission that a specified solar proton flux level is exceeded. These time intervals can be viewed as the periods during which an instrument or system may not operate reliably. Corresponding flux-energy spectra bounding the expected periods of unreliability are then constructed. This is done for both spacecraft incident protons and for shielding levels that are appropriate for modern spacecraft. The results complement currently available models for solar protons used for spacecraft design.

II. Methods

A. Data Base

The solar proton flux data used for this study span a 36 year

Manuscript received September 16, 2011. Revised manuscript received January 20, 2012. This work was supported in part by the NASA Goddard Space Flight Center Internal Research and Development Program.

M. A. Xapsos is with NASA Goddard Space Flight Center, Greenbelt, MD 20771 USA (e-mail: Michael.A.Xapsos@nasa.gov).

C. A. Stauffer is with MEI Technologies, Seabrook, MD 20706 USA.

T. M. Jordan is with EMPC, Gaithersburg, MD 20885 USA.

J. H. Adams, Jr. is with NASA Marshall Space Flight Center, Huntsville, AL 35812 USA.

W.F. Dietrich is a consultant for the Naval Research Laboratory, Washington DC 20375 USA.

period from November 1973 through October 2009. Given a conventional 7-year definition of solar maximum during a solar cycle [3] this represents exactly 21 total years during solar maximum and 15 total years during solar minimum. The first 28 years were during a time period when the Goddard Medium Energy (GME) instrument on the Interplanetary Monitoring Platform-8 (IMP-8) spacecraft operated nearly continuously [12]. The IMP-8 spacecraft orbit was a near circular one at approximately 35 Earth radii and was therefore well positioned to measure interplanetary particle fluxes. The GME data have a proton energy range from 0.88 to 485 MeV divided into 29 non-overlapping energy bins. These data have been supplemented with data obtained from the Geostationary Operational Environmental Satellites (GOES) beginning in 1986. The reason is that the GME instrumentation saturates during very high flux levels while the GOES instrumentation performs better in this regard. Reference 12 gives the details of how these data sets were combined so the best features of each could be taken advantage of. Thereafter the IMP-8 data became intermittent and the spacecraft was eventually de-commissioned.

For the last approximately 8 years the Space Environment Monitors (SEM) on the GOES-8 and GOES-11 spacecraft were used as data sources. Due to both the GOES orbit and the SEM design these solar proton flux measurements are not as accurate as those obtained with the scientific instrumentation on the IMP-8 spacecraft. Thus, the GOES-8 SEM was calibrated against the GME instrument measurements during the approximately 4-year period beginning in 1998 through the end of the GME data. Since the GOES-8 data end in May 2003 and the GOES-11 data begin in June 2003 it was not possible to directly cross calibrate these two similar instruments. Thus, it was assumed that the same calibration factors applied to the GOES-11 SEM that were obtained for the GOES-8 SEM. Examination of the GOES-11 energy spectra with and without these corrections indicated that they were reasonable and resulted in improvements.

B. Model Calculations

This model is based on relatively straight forward, although computationally intensive, direct analyses of the solar proton flux time series (flux vs. time measurements) in the 36-year data base that has been developed. The direct analysis of the time series avoids some of the usual difficulties that are encountered when constructing probabilistic solar particle event models. One such difficulty is the unavoidably arbitrary definition of an event, including start and stop times. This can be particularly difficult when there are several rises and falls in the flux values before the flux returns to the background rate. Once events are defined it is commonly assumed that they are independent of one another, although this may not be the case [1].

The above difficulties are avoided in the current analyses. The approach is to choose a time period during the solar cycle corresponding to the mission of interest and evaluate the amount of time during this period that a pre-determined flux level is equaled or exceeded. This is done for both the total time and the longest continuous time that flux level is equaled or exceeded. The flux level is then incremented and the calculation repeated. This is continued until the maximum observed flux for that time period is reached. In order to combine data from different solar cycles, time periods are referenced to the peak period of each solar cycle as determined by the maximum sunspot number. This is taken as 1968.9, 1979.9, 1989.9 and 2000.2 for the last 4 cycles. The above procedure is repeated for all energies in the time series of flux values. The integral energy spectra of the data base range from > 0.88 to > 327 MeV.

These results are most useful for mission planners if they are determined for different shielding levels. For lightly shielded and heavily shielded applications, "worst case" fluxes may arise from different events. It is therefore useful to transport the time series of energy spectra through various shielding thicknesses before the flux levels are evaluated according to the procedure outlined above. Transport calculations were done whenever at least one energy bin had a flux level above background during a 30-minute measurement period. This was done using the NOVICE code [13] for a shielding thickness range of 50 to 500 mils in solid aluminum sphere geometry. Calculations for the amount of time that specified flux levels were equaled or exceeded during the period of interest were then repeated for each shielding level.

C. Uncertainties

The total amount of time, T, that a specified flux level is exceeded during a mission depends on two quantities. The first is the number of occurrences exceeding that level and the second is the amount of time each occurrence remains above that level. An estimate of the uncertainty can be obtained by assuming this is a compound Poisson process, i.e., a process where the number of occurrences above a given flux, N, is Poissonian and the amount of time each occurrence remains above that level, t, is a random variable. The variance of T is then given by

$$\sigma_T^2 = N \cdot \langle t^2 \rangle \tag{1}$$

where σ_T is the standard deviation of T and $\langle t^2 \rangle$ is the second moment of t [14]. The second moment can be expressed in terms of its mean, $\langle t \rangle$, and its standard deviation, σ_t.

$$\langle t^2 \rangle = \langle t \rangle^2 + \sigma_t^2 \tag{2}$$

The standard deviation of T can then be found by substituting equation (2) into equation (1).

$$\sigma_T = \sqrt{N(\langle t \rangle^2 + \sigma_t{}^2)} \tag{3}$$

The 3 quantities on the right-hand side of equation (3) can be evaluated for a given flux level. Results are shown in figures 1 and 2 as plus or minus one standard deviation on data points. Note that this uncertainty is not defined for the situation where the total time above a given flux is determined by a single occurrence. It should also be noted that the assumption of Poisson time dependence is made only for the purpose of this uncertainty calculation. It is not assumed for any other

presented results.

III. Results

A. Total Time Periods

Results can be obtained for any start and stop time during the solar cycle. Due to the large number of possibilities, results shown are restricted to the solar maximum and solar minimum periods. A conventional definition is used where solar maximum is assumed to be the 7-year period consisting of 2.5 years prior and 4.5 years after the time of the peak sunspot number [3], the latter of which is given in section IIB for solar cycles 20-23. The solar minimum period is the remaining time during each solar cycle. Calculations were done as described in the previous section. Results presented here incorporate either the entire 21 years of data measured during solar maximum or the entire 15 years of data measured during solar minimum.

Figure 1 is a plot of the total number of hours per solar maximum year that the proton flux equals or exceeds the value shown on the x-axis in units of protons per square centimeter per second per steradian. Note that the y-axis value is not a continuous time period. It was determined by summing the distinct periods during the 21 years of solar maximum data, and so represents the mean of the total time per year of operation during solar maximum when the flux threshold is exceeded. These results have been divided by 21 years so the normalized data could be compared to solar minimum. The flux range shown in the figure extends 2 orders of magnitude down from the maximum flux for each energy bin. As an example suppose one is interested in the > 11.1 MeV energy bin. It is seen that a flux level of 10^4 p/(cm^2-s-sr) is exceeded about 2 hours per year on average while a flux level of 10^3 is exceeded about 1 day per year on average during solar maximum. Note that the continuous range of information available from this analysis is more complete than that obtained from analysis of a single worst case situation. This lends itself to evaluation of reliable periods of operation of spacecraft instrumentation.

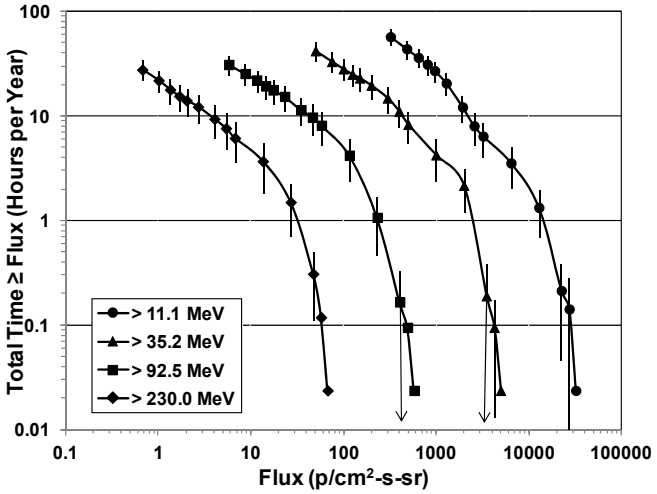

Fig. 1. Total number of hours per year during solar maximum that the proton flux equaled or exceeded the value shown on the abscissa for 4 energy groups: > 11.1, > 35.2, > 92.5 and > 230 MeV. Results are for surface incident fluxes. Error bars indicate plus or minus one standard deviation. An arrow indicates the uncertainty extends down to zero. See text.

The results displayed in figure 1 can be compared to those shown in figure 2 for solar minimum. It is generally seen that the same y-axis values occur at lower fluxes during solar minimum, as would be expected. For example, the > 11.1 MeV energy bin shows that fluxes are approximately an order of magnitude lower during solar minimum. Although the solar minimum results do not represent worst case situations in general they may be useful for missions that occur entirely during this period of time.

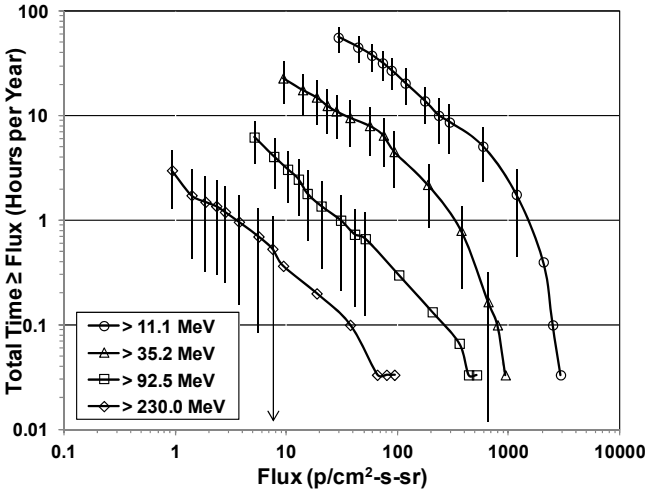

Fig. 2. Total number of hours per year during solar minimum that the proton flux equaled or exceeded the value shown on the abscissa for 4 energy groups: > 11.1, > 35.2, > 92.5 and > 230 MeV. Results are for surface incident fluxes. Error bars indicate plus or minus one standard deviation. An arrow indicates the uncertainty extends down to zero. See text.

Up to this point results shown have been for unshielded incident protons. As discussed before these results would be more useful if they were calculated for different levels of shielding. Thus, proton transport calculations were done for each 30 minute long energy spectrum in the 36 year data base whenever fluxes were above background. This was done for 50, 100, 200, 300 and 500 mils (1.27, 2.54, 5.08, 7.62, and 12.7 mm) of aluminum shielding in solid sphere geometry. Attenuated fluxes were grouped into the same energy bins as the incident fluxes. This resulted in 36-year long time series for both incident and attenuated flux values for the same energy groups. Example results for solar maximum are shown in figures 3-5 for > 11.1, > 35.2 and > 92.5 MeV protons. It is seen that in all cases results are noticeably affected by the amount of shielding present. For example, the > 35.2 MeV flux level at 10^3 p/(cm^2-s-sr) was equaled or exceeded for 4.2 hours per year without shielding, 1.6 hours per year with 200

mils of Al and about 0.1 hour per year with 500 mils of Al shielding. Examination of the figures clearly shows that the differences between the unshielded and shielded cases are more pronounced for low energies than for high energies. It should also be noted that the results obtained do not always yield perfectly smooth curves. As the value of flux increases along the x-axis, the calculated time value can undergo a sudden decrease as events are no longer counted within that flux range. However, the data base does contain enough events to smooth out the results quite a bit.

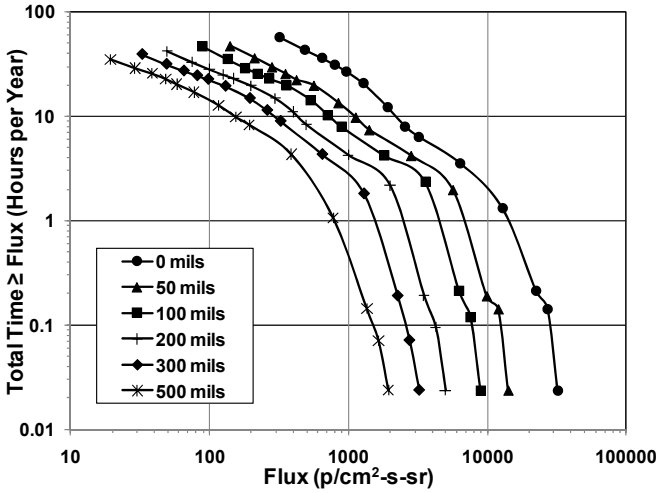

Fig. 3. Total number of hours per year during solar maximum that the proton flux equaled or exceeded the value shown on the abscissa for > 11.1 MeV protons with 0, 50, 100, 200, 300 and 500 mils of aluminum shielding in solid sphere geometry.

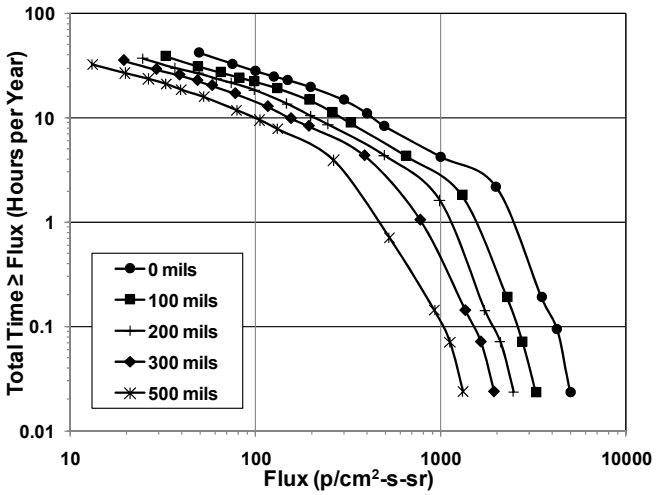

Fig. 4. Total number of hours per year during solar maximum that the proton flux equaled or exceeded the value shown on the abscissa for > 35.2 MeV protons with 0, 100, 200, 300 and 500 mils of aluminum shielding in solid sphere geometry.

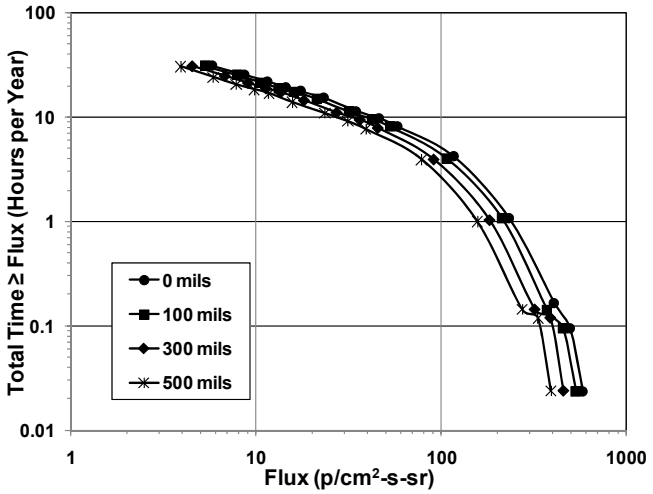

Fig. 5. Total number of hours per year during solar maximum that the proton flux equaled or exceeded the value shown on the abscissa for > 92.5 MeV protons with 0, 100, 300 and 500 mils of aluminum shielding in solid sphere geometry.

Since this methodology has generated a lot of results it is of interest to look for a more compact way to view them. One possibility is to calculate a flux vs. energy spectrum for a given time period. As an example, suppose a mission can afford to lose only one hour of data per solar maximum year due to high intensity solar proton fluxes. A proton flux vs. energy plot for the one hour per year period can be constructed using results such as those shown in figure 1. The various flux levels corresponding to a y-axis value of 1 hour per year are determined for each energy group. A plot of flux vs. energy can then be made as shown in figure 6 for the unshielded case. Each point on this plot represents the flux for the corresponding energy bin that will be exceeded one hour per year on average. This 1-hour per year value holds only for individual points on the curve. It is not the case that the spectrum as a whole is exceeded 1 hour per year. As such the results can be viewed as a worst case flux vs. energy spectrum that defines the 1-hour data loss criterion. Results for the shielded cases were obtained in a similar fashion and are also shown in figure 6. This is a particularly attractive representation because of its compactness as well as its similarity to measured solar proton event spectra.

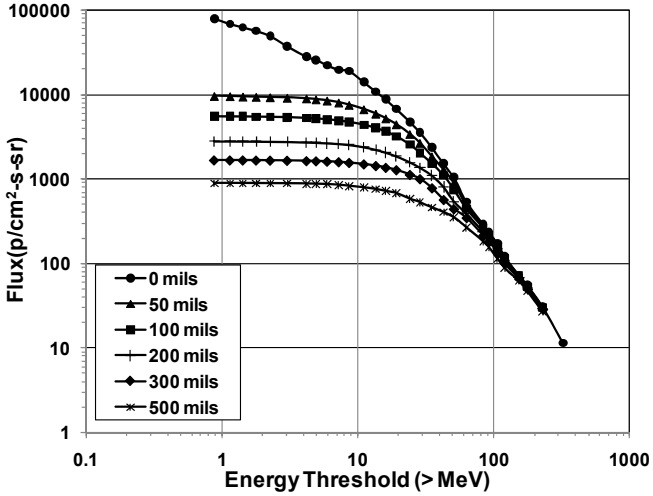

Fig. 6. Flux vs. proton energy spectra for a 1-hour per year data loss during solar maximum. See text for interpretation. Results are shown for 0, 50, 100, 200, 300 and 500 mils of aluminum shielding.

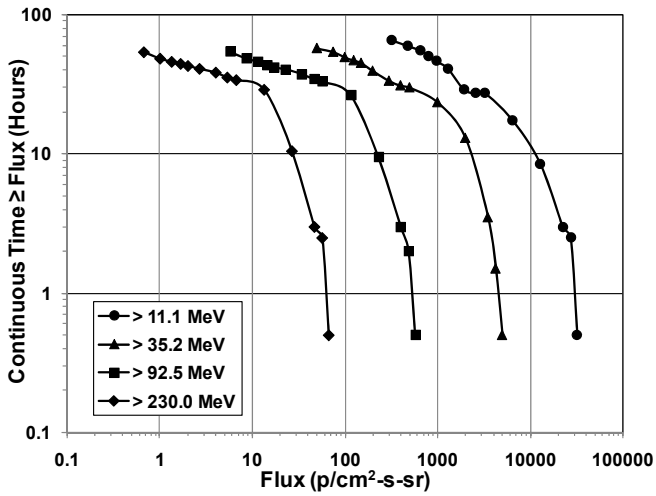

Fig. 7. Worst case number of continuous hours during solar maximum that the proton flux equaled or exceeded the value shown on the abscissa for 4 energy groups: > 11.1, > 35.2, > 92.5 and > 230 MeV. Results are for surface incident fluxes.

B. Continuous Time Periods

If the supposition is accepted that a system or instrument does not operate reliably beyond some flux threshold, then there are two important considerations that need to be evaluated. The first is the *total* time during the mission that flux threshold is exceeded. That was discussed in the previous section. The second is the longest *continuous* time during the mission that threshold is exceeded. In the case of an instrument this would represent a worst case scenario of how long it could spend in a continuous state of unreliable operation. For example, this might occur when an imager is flooded with noise caused by the high proton flux.

Figures 7 and 8 show results for the longest continuous time period that the flux value on the x-axis is equaled or exceeded. Calculations for figure 7 were done for the 21 years of solar maximum data while those for figure 8 were done for the 15 years of solar minimum data. Much like the situation shown in the previous section it is seen that for a given flux level, the y-axis values are noticeably greater during the solar maximum period.

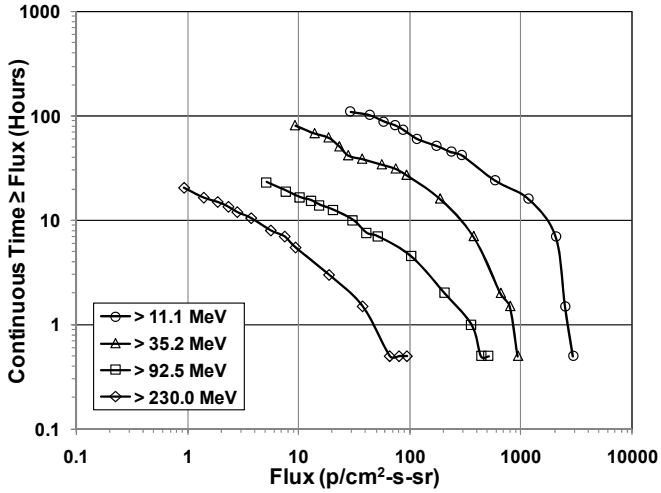

Fig. 8. Worst case number of continuous hours during solar minimum that the proton flux equaled or exceeded the value shown on the abscissa for 4 energy groups: > 11.1, > 35.2, > 92.5 and > 230 MeV. Results are for surface incident fluxes.

It is also desirable to construct worst case flux vs. energy spectra for a given time window. The results shown in figure 7 represent the longest continuous time interval that the flux equals or exceeds a value. Thus, it does not necessarily represent the worst case fluence for the time window when there are successive rises and falls in the flux values during a solar event. Worst case spectra must be derived by first selecting a shielding thickness and energy bin. A time window with a fixed width is then moved across the entire time series, one 30-minute increment at a time, to evaluate the maximum fluence seen at any position in the time series during that time window. This subtle distinction from using results such as those in figure 7 becomes more important as longer time windows are considered. Results are shown in figures 9 and 10 for 1-hour and 24-hour time windows during solar maximum, respectively. Since each data point in the figures is calculated independently, this leaves open the

possibility that different points could result from different solar proton events. For the results shown in figure 9, however, all data turned out to come from the well known event of October 1989. This is consistent with the use of this event by the CREME96 suite of codes as worst case. On the other hand, for the worst case 24 hour period shown in figure 10, the spectra are made up of data from 3 separate events. This includes the events of July 2000 and November 2000 along with the October 1989 event. As can be seen in the figure, the October 1989 event contributes the worst case fluxes at energies greater than about 50 MeV while the other 2 events make up the majority of the spectra at lower energies. Thus, while the October 1989 event is often a suitable choice as a worst case situation, this may not always be true. For example, some highly scaled technologies are susceptible to single event upset by protons close to their end of range [15]. For this situation one of the events that occurred in the year 2000 would represent a worst case flux. The particular choice would depend on the level of shielding. Finally, it is worth noting that a comparison of figures 9 and 10 indicates how much the worst case flux levels vary when the time window is reduced from 1 day to 1 hour.

The fact that different events contribute to the results shown in figure 10 indicates that these results are continuously evolving. Due to the limited data available it is reasonable to ask how much the flux levels would change as subsequent solar cycles are included in the data base. Since only extreme intensity events could alter figures such as 9 and 10 it is reasonable to see what can be gleaned from historical-type evidence to address this. Constraints on the upper limit of solar proton event sizes have been determined from fluctuations of ^{14}C observed in tree rings over a long period of time [16] and measured radioactivity in lunar rocks brought back during the Apollo missions [17]. However, the strictest constraint comes from analysis of approximately 400 years of the nitrate record in polar ice cores, indicating the largest event over this time period was estimated to be 1.9×10^{10} cm^{-2} for > 30 MeV protons [18]. This is known as the Carrington Event, which occurred in 1859. The fact that the event which occurred in October 1989 is approximately within a factor of 2 of the magnitude of the Carrington Event indicates that larger events are possible but events that are orders of magnitude larger than the October 1989 event are highly unlikely. In fact, a design upper limit for the magnitude of an event was derived from satellite data using a parametric bootstrap technique [19] that is consistent with the magnitude of the Carrington Event before the Carrington Event size was known [8]. Thus, indications are that figures 9 and 10 will change with the addition of subsequent solar cycle data but probably not drastically.

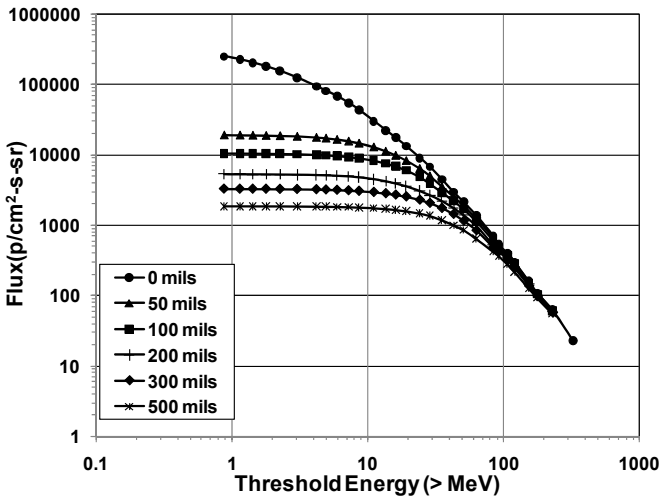

Fig. 9. Worst case flux vs. proton energy spectra for a 1-hour time window during solar maximum. Results are shown for 0, 50, 100, 200, 300 and 500 mils of aluminum shielding. Each data point comes from the October 1989 event.

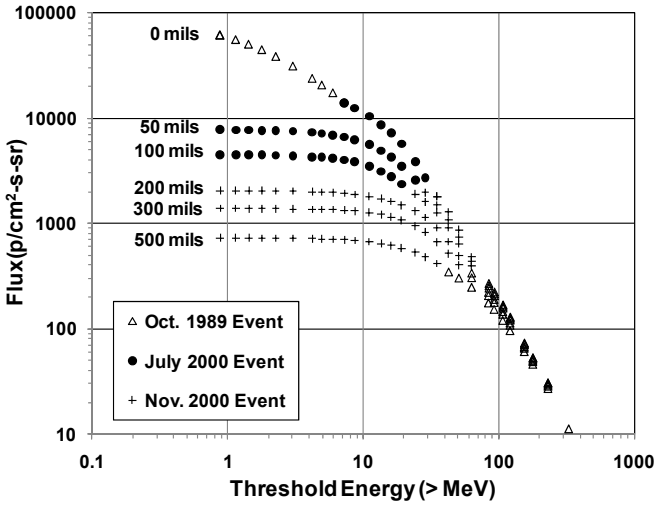

Fig. 10. Worst case flux vs. proton energy spectra for a 24-hour time window during solar maximum. Results are shown for 0, 50, 100, 200, 300 and 500 mils of aluminum shielding. The event that each worst case point comes from is shown in the legend.

IV. Summary and Conclusions

This paper has presented analyses of high intensity solar proton fluxes that are free from many of the assumptions that are made for statistical models of solar proton events. Results show the amount of time that high intensity solar proton flux levels are expected to be equaled or exceeded during the entire mission and during a single continuous period. Analyses have been done for the time series of flux values transported through varying shield thicknesses, making the results more relevant for spacecraft applications. From these results, worst case flux vs. energy spectra have been derived that can be used by designers to bound periods of unreliable operation of space systems and instrumentation. This is a natural way to

tie the results to design goals of projects, especially those of data requirements for instrumentation.

REFERENCES

[1] M. A. Xapsos, C. Stauffer, J.L. Barth and E.A. Burke, "Solar Particle Events and Self-Organized Criticality: Are Deterministic Predictions of Events Possible?", IEEE Trans. Nucl. Sci., Vol. 53, no. 4, 1839-1843 (Aug. 2006).

[2] J.H. King, "Solar Proton Fluences for 1977-1983 Space Missions", J. Spacecraft, Vol. 11, 401-408 (1974).

[3] J. Feynman, G. Spitale, J. Wang and S. Gabriel, "Interplanetary Fluence Model: JPL 1991", J. Geophys. Res., Vol. 98, 13281-13294 (1993).

[4] M.A. Xapsos, G.P. Summers, J.L. Barth, E.G. Stassinopoulos and E.A. Burke, "Probability Model for Cumulative Solar Proton Event Fluences", IEEE Trans. Nucl. Sci., Vol. 47, No. 3, 486-490 (June 2000).

[5] R.A. Nymmik, "Probabilistic Model for Fluences and Peak Fluxes of Solar Energetic Particles", Radiation Mesurements, Vol.30, 287-296 (1999).

[6] M. A. Xapsos, C. Stauffer, T. Jordan, J.L. Barth and R.A. Mewaldt, "Model for Cumulative Solar Heavy Ion Energy and Linear Energy Transfer Spectra", IEEE Trans. Nucl. Sci., Vol. 54, 1985-1989 (Dec. 2007).

[7] M.A. Xapsos, G.P. Summers and E.A. Burke, "Probability Model for Peak Fluxes of Solar Proton Events", IEEE Trans. Nucl. Sci., Vol. 45, 2948-2953 (1998).

[8] M.A. Xapsos, G. P. Summers, J.L. Barth, E.G. Stassinopoulos and E.A. Burke, "Probability Model for Worst Case Solar Proton Event Fluences", IEEE Trans. Nucl. Sci., Vol. 46, 1481-1485 (1999).

[9] A.J. Tylka et al., "CREME96: A Revision of the Cosmic Ray Effects on Microelectronics Code", IEEE Trans. Nucl. Sci., Vol. 44, 2150-2160 (1997).

[10] K.A. Ryden et al., "Observations of Internal Charging Currents in Medium Earth Orbit", IEEE Trans. Plasma Sci., Vol. 36, No. 5, 2473-2481 (Oct. 2008).

[11] H.D.R. Evans, P. Buhler, W. Hajdas, E.J. Daly, P. Nieminen and A. Mohammadzadeh, "Results from the ESA SREM Monitors and Comparison with Existing Radiation Belt Models", Adv. Sp. Res., Vol. 42, No. 9, 1527-1537 (Nov. 2008).

[12] M.A. Xapsos, C. Stauffer, G.B. Gee, J.L. Barth, E.G. Stassinopoulos and R.E. McGuire, "Model for Solar Proton Risk Assessment", IEEE Trans. Nucl. Sci., Vol. 51, 3394-3398 (2004).

[13] T. M. Jordan, "An Adjoint Charged Particle Transport Method", IEEE Trans. Nucl. Sci., Vol. 23, no. 6, 1857-1861 (Dec. 1976).

[14] E.A. Burke and G.P. Summers, "Extreme Damage Events Produced by Single Particles", IEEE Trans. Nucl. Sci., Vol. 34, 1575-1579 (Dec. 1987).

[15] D.F. Heidel et al., "Single Event Upsets and Multiple Event Upsets on a 45 nm SOI SRAM", IEEE Trans. Nucl. Sci., Vol. 56, 3499-3504, Dec. 2009.

[16] R.E. Lingenfelter and H.S. Hudson, "Solar Particle Fluxes and the Ancient Sun" in *Proc. Conf. Ancient Sun*, edited by R.O. Pepin, J.A. Eddy and R.B. Merrill, Pergamon Press, London, pp.69-79 (1980).

[17] R.C. Reedy, "Radiation Threats from Huge Solar Particle Events", in *Proc. Conf. High Energy Radiat. Background in Space*, edited by P.H. Solomon, NASA Conference Publication 3353, pp.77-79 (1997).

[18] K.G. McCracken, G.A.M. Dreschoff, E.J. Zeller, D.F. Smart and M.A. Shea, "Solar Cosmic Ray Events for the Period 1561 – 1994 1. Identification in Polar Ice", J. Geophys. Res., Vol. 106, 21585-21598 (2001).

[19] B. Efron and R.J. Tibshirani, *An Introduction to the Bootstrap*, Chapman & Hall, NY, 1993.